Optical Materials 111 (2021) 110569

Contents lists available at ScienceDirect

Optical Materials

journal homepage: http://www.elsevier.com/locate/optmat

Study on the bio-inspired electrochromic device enabled via dielectric elastomer actuator

Pengfei Zhao [a,b,c], Yong Cai [b], Chen Liu [a,b], Dengteng Ge [d], Bo Li [b,*], Hualing Chen [a,b,**]

[a] State Key Laboratory for Strength and Vibration of Mechanical Structures, Xi'an Jiaotong University, Xi'an, 710049, PR China
[b] Shaanxi Key Laboratory of Intelligent Robots, School of Mechanical Engineering, Xi'an Jiaotong University, Xi'an, 710049, PR China
[c] Department of Mechanical Engineering, Taiyuan Institute of Technology, Taiyuan, 030008, PR China
[d] Institute of Functional Materials, Research Institute of Donghua University, Donghua University, Shanghai, 201620, PR China

ARTICLE INFO

Keywords:
Dielectric elastomer actuator
Stretchable photonic crystal
Strain sensing
Electrochromic device
Structural color
Color change

ABSTRACT

As a promising research field, electrochromic devices have attracted researcher's attention because of their dynamic display capabilities, high brightness, and convenience of electric signals. Among all the electrochromic modes, the use of electroactive actuators to produce color change is one of the important means. In view of the characteristics of dielectric elastomer (DE) materials such as rapid response and large deformation under electric signal, dielectric elastomer actuators (DEAs) were prepared and explored for their applications in biomedicine, aerospace, intelligent robotics and other fields. In this paper, inspired by the skin of chameleons, a kind of electrochromic device enabled via dielectric elastomer actuator (EDDEA) is prepared by integrating the stretchable photonic crystals (SPCs) with DEAs. The SPCs can achieve color changes in visible light range and maintain stable performance during multiple working cycles. The prepared EDDEA can produce strain under an electric field, which in turn causes color changes. In addition, the EDDEA can be used to display and measure the strain range of the DEA during actuating process under the excitation of electric field. The results demonstrate that the prepared EDDEA is a fully flexible, highly integrated electrochromic device, which can produce a wide range of color change under electric field. Meanwhile, this device provides potential application value in the strain range control of DEAs.

1. Introduction

Soft actuator is a new type of actuators made of soft materials. Compared with traditional rigid actuators such as electric motors, soft actuators such as dielectric elastomer actuators (DEAs), ionic polymer metal composites (IPMCs), and shape memory alloys (SMAs) have better flexibility and greater energy density, which are similar to biological muscles. Therefore, these soft actuators are called artificial muscles. Using artificial muscle to actuate the light-small robots can effectively reduce the size and complexity of the structures while generating effective actuating force, improving the compactness and integration of robots. As an electroactive soft actuator, the dielectric elastomer actuator (DEA) is a typical representative of artificial muscle, which can produce large deformation under the excitation of electric field. A DEA is composed of flexible electrodes and a dielectric layer sandwiched by the flexible electrodes, which shrinks in thickness and expands in area when subjected to an applied voltage in the direction of thickness (see Fig. 1.). DEA is characterized by high energy density, excellent flexibility, compact structure, simple excitation, large strain, good flexibility, light weight, stable chemical structure, no need for liquid environment, low price, etc., which shows excellent comprehensive performance among various soft actuators. Therefore, researchers have devoted to the research fields of the performance characteristics, function realization and application of DEAs, and have recently developed a considerable number of applications, such as soft actuators [1–3], energy harvesting device [4,5], underwater robots [6,7], etc.

The main driving modes of DEAs are in-plane isotropic deformation, pure shear deformation (see Fig. 1.), out of plane deformation, etc. Among these driving modes, pure shear DEAs adopt the way of pre-stretched and fixed in one direction, while staying free in the vertical direction. This simple structure can produce unidirectional actuating with large deformation, which is considered as an ideal soft actuator. A

* Corresponding author.
** Corresponding author.State Key Laboratory for Strength and Vibration of Mechanical Structures, Xi'an Jiaotong University, Xi'an, 710049, PR China.
E-mail addresses: liboxjtu@xjtu.edu.cn (B. Li), hlchen@mail.xjtu.edu.cn (H. Chen).

https://doi.org/10.1016/j.optmat.2020.110569
Received 22 July 2020; Received in revised form 8 September 2020; Accepted 20 October 2020
Available online 26 October 2020
0925-3467/© 2020 Elsevier B.V. All rights reserved.

dielectric elastomer is susceptible to modes of instabilities in the actuation process. When the voltage rises up, the membrane thins down, so the same voltage produces a higher electric field which will further squeeze the membrane as a positive feedback till the electrical breakdown [8]. This failure mode, named pull-in instability, is considered as the key issue that hinders the realization of large stable deformation [9]. Pull-in instability can be understood as follows: When the applied voltage exceeds a critical level, the electrostatic stress due to the voltage prevails in the elastic stress due to the deformation of the elastomer. Therefore, the elastomer membrane becomes even thinner, leading to an increase in the electric field since the voltage is kept constant, which in turn further compresses the membrane. The significant growth of the electrostatic stress causes the film to expand drastically without the balance of elastic stress, until the electrical breakdown [10]. Pull-in was frequently observed in the equal biaxial mode, but in other modes, the stability behavior is different. DEA in the pure shear-mode features a large strain without pull-in, as its unique advantage is that it offers a new route for achieving giant deformation [11–14]. In this paper, the pure shear DEAs is taken as the research object.

Recently, stretchable photonic crystals (SPCs) have attracted many researchers attention owing to its deformability and color change ability, which become many hot fields in academia such as flexible display [15–40], information encryption [41–44], human assistance [45–52], colorful sensors [53–64], etc. The colors of SPCs belong to structural colors, which have the characteristics different from the common chemical colors. The structural color is produced by a new type of optical system that achieves color display and color change through the optical interference. In fact, there have been various creatures in nature that reflect colorful bodies through structural colors, such as chameleons and beetles, etc. [65–71] In addition to displaying structural color, the SPC can also produce color change through its large deformation, so the structural color of SPCs can be regulated and more vivid colors can be displayed. Scientific research shows that the color change mechanism of chameleon belongs to the structural color change. When stimulated, the melanophore layer of the chameleon is deformed by the muscle actuating, causing the iridophore layer to be deformed. The iridophore layer itself is a functional layer with structural color which is caused by the crystals arranged in the layer. As shown in the biological mechanism in Fig. 1a, the deformation of the iridophore layer caused by muscle contraction will lead to changes in the parameters of x, y, D, resulting in structural color change. That is, the colors of chameleon skin corresponds to the deformation of muscle. Inspired by the integration of actuating and color changing function in biological tissue, we believe that the combination of a DEA and a SPC can form an integrated electrochromic device which combines the functions of deformation as well as color change just like the chameleon skin.

In this work, inspired by the skin of chameleons, an electrochromic device enabled via dielectric elastomer actuator (EDDEA) is prepared by integrating the pure shear DEAs with the stretchable photonic crystals (SPCs). Firstly, a pure shear DEA was prepared and its mechanical properties as well as actuating performance under an electric field are studied. Subsequently, an SPC with hexagonally arranged air columns was prepared, which has the advantages of wide color changing range (180 nm), small Young's Modulus, and good color changing stability (2000 cycles). Based on the properties of the proposed pure shear DEAs and SPCs, the integrated structure of the SPC and DEA was designed and fabricated, obtaining the EDDEA (see Fig. 1b and c.) which can produce color change in visible light range from red to blue under an electric field (see Fig. 1d.). After that, the electrochromic property of EDDEA was studied and the relationship between applied voltage, strain range, and structural colors was also analyzed. When the voltage ranging from 3.5 kV to 6.5 kV applied to the prepared EDDEA, a strain up to 30% occurred and a wide range of color change came up corresponding to the strain ranges. Finally, the application of the EDDEA was explored in the strain sensing of DEA by a group of comparative experiments, which validates the potential value of EDDEA in the strain sensing of soft actuators.

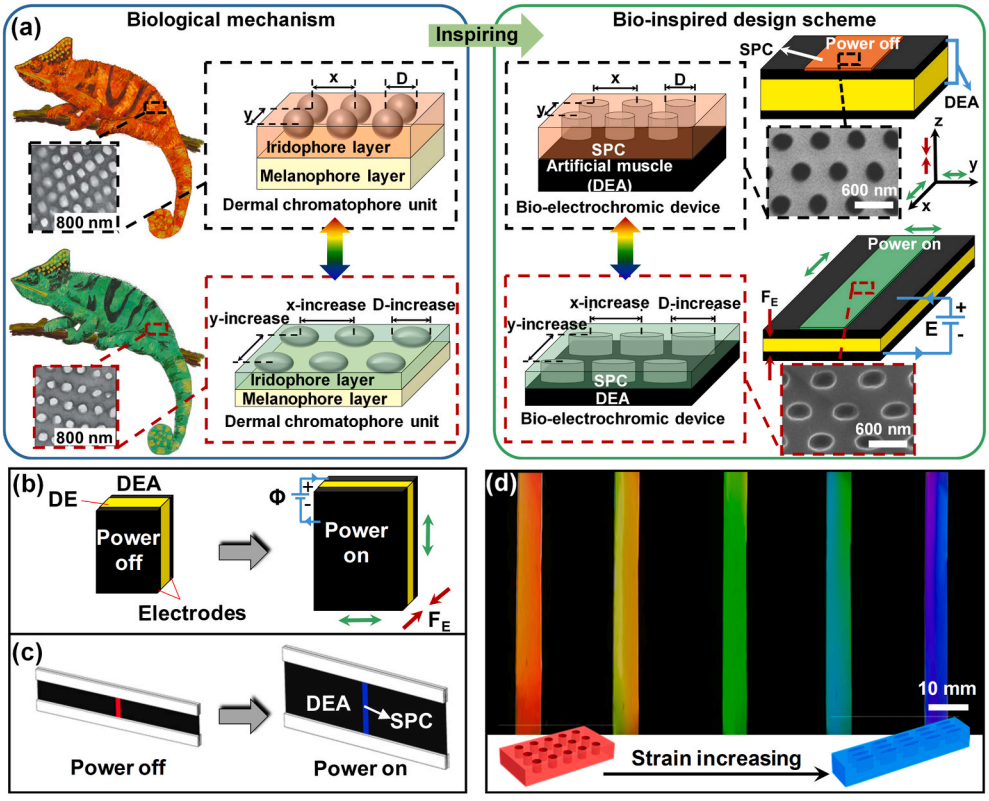

Fig. 1. Schematic diagram of the electrochromic device enabled via dielectric elastomer actuator (EDDEA). (a) Bio-inspired design scheme of the EDDEAs. F_E is the electric field force between two electrodes. (b) Schematic actuating mechanism of dielectric elastomer actuators. (c) The electrochromic mechanism of EDDEAs. (d) Optical photographs of the vivid colors of an SPC. The color is red when no strain is applied, and successively changes to yellow, green, light blue, and blue as the strain increases. (For interpretation of the references to color in this figure legend, the reader is referred to the Web version of this article.)

2. Experimental section

2.1. Materials and characterizations

VHB 4910 (3 M, Saint Paul, Minnesota, USA), nanoimprint resist (ultraviolet cured polymer, Ormostamp, Micro Resist Technology, Germany), and silicone rubber adhesive (Sil-Poxy, Smooth-on, Inc., USA) were used as received. SPC was made of Polydimethylsiloxane (PDMS, Dow Corning Sylgard 184, USA) with part A and B at a mass ratio of 10:1.

A field emission scanning electron microscope (Gemini SEM 500, Zeiss, Germany) was used to obtain scanning electron microscope (SEM) images. An angle-resolved spectrum system (R1, Ideaoptics, China) and the spectrometer (NOVA, Ideaoptics, China) were used to measure the reflectance spectrum. A laser displacement sensor (IL-065, Keyence, Japan) is used to measure the deformation of EDDEA, and the strain as well as the relationship between the strain of DEA and the reflectance spectra of SPC can be obtained. The tensile testing machine (ZQ-60B, Zhiqu, China) is used to measure the relationship between the stretching force and the strain.

2.2. Preparation of SPCs

The detailed preparation process of SPCs is shown in Fig. 2a. Step one, we obtained a template for the preparation of SPCs by turning mold on the silicon wafer (area of 50 × 50 mm^2, depth of 500 nm, period of 600 nm, diameter of 300 nm) purchased from Eulitha AG, Switzerland (see Fig. 2c, d, e.). Step two, we mixed the components A and B of PDMS at the mass ratio of 10:1 by stirring, and then coated the mixture onto the template prepared in step one after vacuum pumping. Finally, the SPCs were obtained after 4 h' heating at 60 °C (see Fig. 2f.). The prepared SPC can exhibit obvious color changes under uniaxially stretching, which caused by the changes of the nanostructure (see Fig. 2g, h, i.). The color change mechanism of the SPC is that the nanostructures change with the deformation of the material, which in turn causes the variation of structural colors. Therefore, it is necessary to study the relationship between the deformation, the nanostructure and the structural color of the SPC [72,73]. When the prepared SPC is uniaxially stretched, the cylindrical holes of the nanostructures become elliptical holes. The diameter of the holes and the distance between the holes of the nanostructures become larger in the stretching direction. Correspondingly, the diameter of the holes and the distance between the holes of the nanostructures become smaller in the direction perpendicular to the stretching, which leads to the variation of the structural color. The details of the variation of nanostructures of the proposed SPC during stretching process can be found in Refs. [74].

2.3. Preparation of DEAs

DEAs was prepared using poly-acrylic films (VHB 4910, 3 M, Minnesota, USA). Firstly, the films were equally stretched biaxially to 4 times the original sizes in horizontal and vertical directions and fixed with an aluminum alloy frame. Afterwards, strip shaped 1 mm thick polymethyl methacrylate (PMMA) frames were installed at the two ends of the film in the Y direction to fix the shape in the X direction, while the shape in the Y direction is not fixed (see Fig. 2j.). The electrodes of conductive silicone rubber (Elastosil LR 3162, Wacker, Germany) were sprayed on the films, and the pure shear DEAs were obtained after 2 h

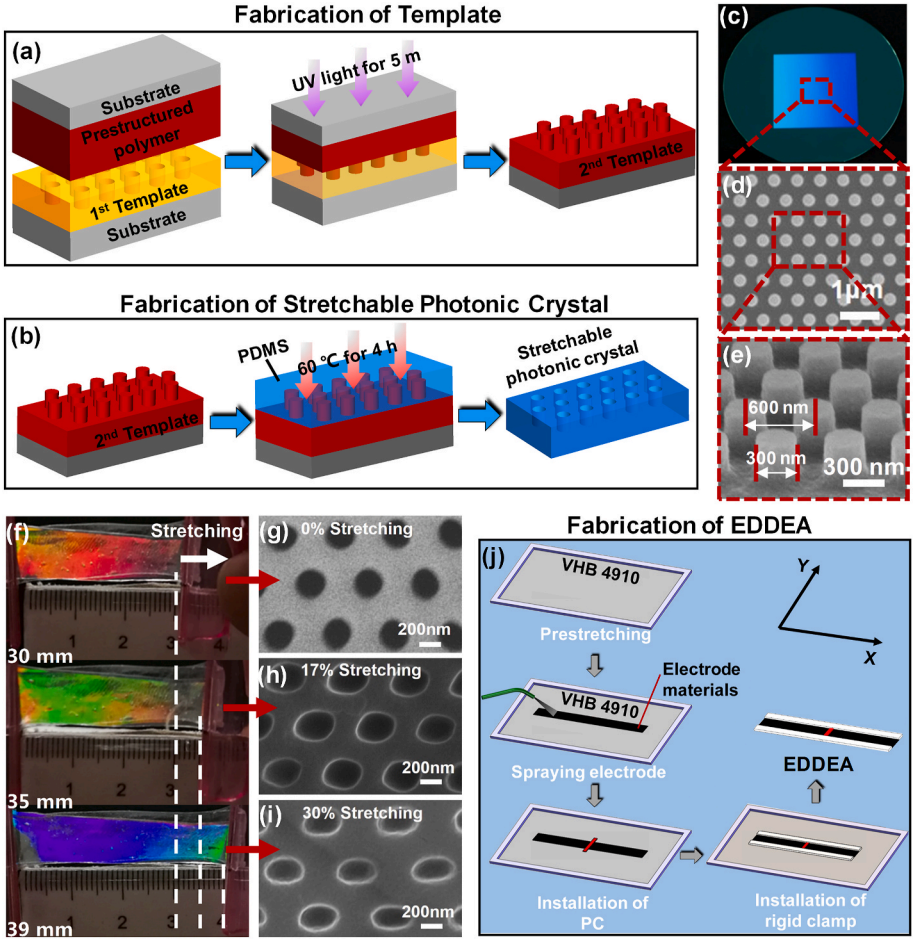

Fig. 2. Fabrication of the SPCs and EDDEAs. (a) Fabrication process of the template. (b) Preparation of the stretchable photonic crystal (SPC). (c) Template with hexagonally arranged columns. Graphical area is 50 × 50 mm^2. (d) SEM image of the template. (e) SEM image of 3D microscopic structure of the template. (f) The sample of SPC and its strain-related color change. (g) SEM image of the sample without strain. (h) SEM image of the sample under 17% stretching strain. (i) SEM image of the sample under 30% stretching strain. (j) Fabrication process of the electrochromic device enabled via dielectric elastomer actuator (EDDEA). (For interpretation of the references to color in this figure legend, the reader is referred to the Web version of this article.)

solidification of the electrodes at 80 °C. Since the deformation in horizontal direction has been limited, the DEA will deform in vertical direction to achieve actuating when an electric field is applied on it.

2.4. Combination of the SPC and the DEA

The fabrication process of the electrochromic device is shown in Fig. 2j. Firstly, Silicone rubber adhesive was uniformly coated on the back of the prepared SPC. Then the SPC was pressed on the surface of DEA with the length direction of SPC consistent with the direction of free deformation (Y direction in Fig. 2j.) of DEA. Subsequently, the integrated EDDEA can be obtained after fixing the position of SPC by PMMA frames and heating at 60 °C for 15 min.

3. Results and discussion

3.1. Matching properties of the DEA and the SPC

During the electrochromic process of the proposed EDDEA, the electrostrictive deformation of the DEA (see Fig. 3a.) causes the stretching strain of the SPC, leading to the color change of the SPC (see Fig. 3b.). That is to say, the strain of DEA is corresponding to the color of the SPC. For this reason, the first step is to study the matching properties of the DEA and the SPC.

In the preparation of DEA, two types of DEA schemes of single-layer VHB and double-layer VHB (see Fig. 3c and d.) were selected and tested. The results show that the DEA with double-layer VHB structure has a higher breakdown voltage and is less prone to accidental damage owing to the greater thickness at the same stretching rate. Therefore, we finally selected the DEA with a double-layer VHB structure for subsequent experiments. For EDDEA, the structural stiffness of the DEA and the overall Young's Modulus of the materials should match the Young's Modulus of the SPC. As shown in Fig. 3e, the stiffness curve as well as the stress-strain curve of DEA were tested under the electric field (5000 V). The general rule of the stiffness curve and the stress-strain curve is consistent, the slope of which goes through a process of decreasing first and then increasing. The decrease of the slope is due to the elastic deformation of DEA, and the subsequent increase of the slope is due to the influence of strain-stiffening. Nevertheless, the slope of the two curves does not change much, and can be regarded as approximately constant,

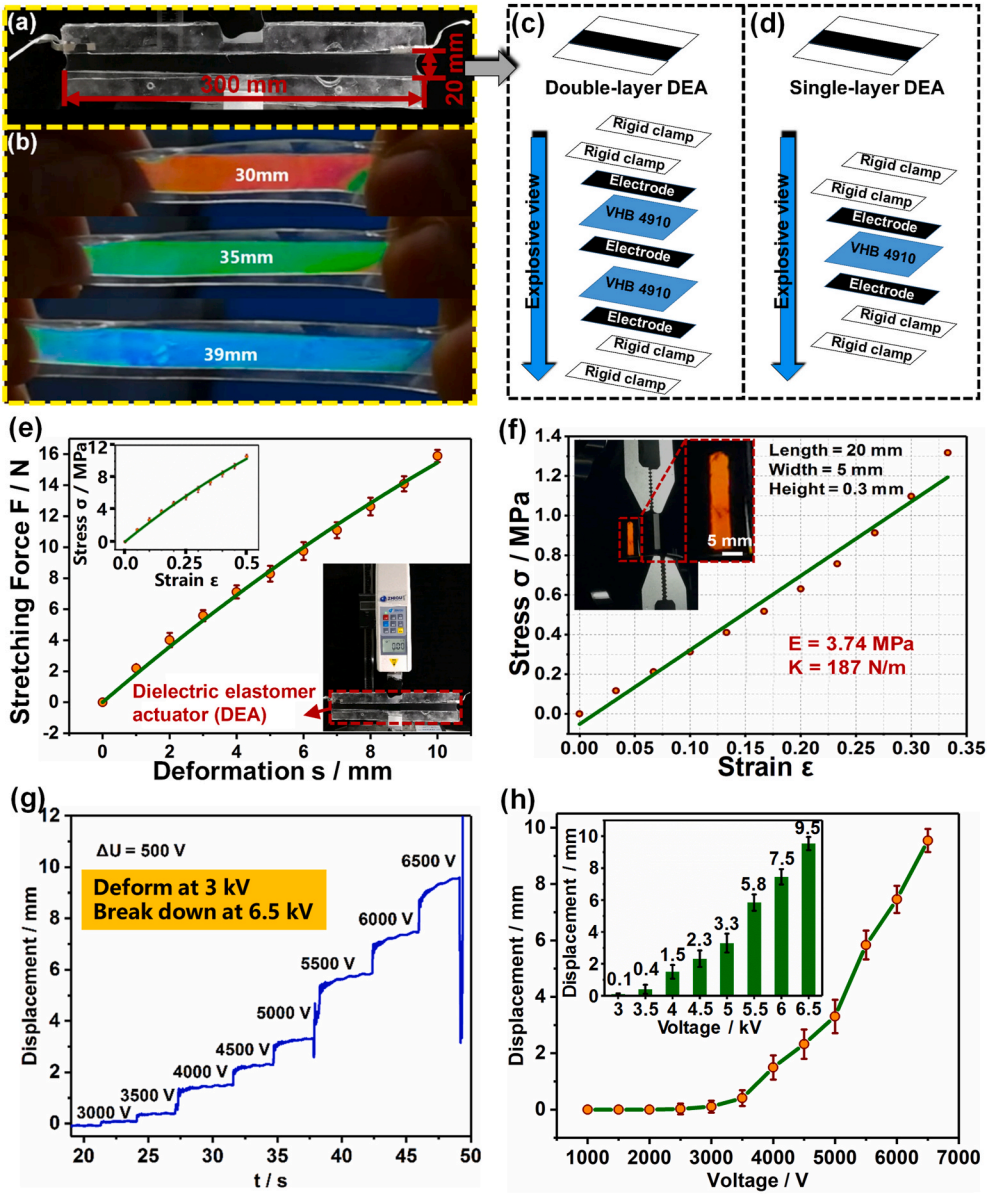

Fig. 3. Matching properties of the SPCs and EDDEAs. (a) An optical photograph of DEA. (b) Optical photographs of the strain-dependent colors of SPCs. (c) Structure of the double-layer DEA. (d) Structure of the single-layer DEA. (e) Stiffness curve and the stress-strain curve of the double-layer DEA. (f) Stress-strain curve of the SPC. (g) Displacement of the free end of DEA under varying voltage from 0 V–6500 V ΔU = 500 V. (h) Relationship between the displacement of the free end of DEA and the applied voltage. The error bars represent the deviations of twelve sets of test data. (For interpretation of the references to color in this figure legend, the reader is referred to the Web version of this article.)

whose average values are 1750 N m^{-1} and 23.26 MPa, respectively. As shown in Fig. 3f, the stress-strain curve of SPC illustrates that the stiffness and Young's Modulus of SPC (3.74 MPa) are smaller than that of DEA (23.26 MPa). This indicates that the SPC will deform with DEA as soon as the electrostrictive deformation of DEA occurs under applied voltage, and the SPC has little effect on the electrostrictive performance of DEA.

Fig. 3g illustrates the displacement of the DEA free end under applied voltage increasing from 0 V to 6500 V (the increase amplitude for each time $\Delta U = 500$ V). It can be seen that the actuator does not deform below 3000 V. When the applied voltage increases to 3000 V, the significant deformation of DEA occurs. When the applied voltage reaches 6500 V, the deformation of DEA reaches its maximum value (9.5 mm), and then breakdown occurs. Fig. 3h shows the relationship between the deformation of DEA and the applied voltage. When the applied voltage increases from 0 V to 6500 V, the deformation of DEA changes from 0 mm to 9.5 mm, and the corresponding strain range is from 0% to 47.5%, which matches the strain range of color change of SPC (>17%, green; > 30%, blue). The above results show that it is feasible to use the color change of SPC to represent the strain of DEA by integrating SPC with DEA.

3.2. Color change performance of the SPC under cyclic mechanical stretching

The ability of color change under cyclic stretching is an important performance of SPCs, which determines the overall performance as well as the possibility of practical application of this kind of materials. Thus 2000 cycles of cyclic stretching tests for SPC were carried out to verify the color change performance of the prepared SPC under cyclic mechanical stretching.

Fig. 4a illustrates the relationship between stress σ and strain ε of the SPC during 2000 cycles of cyclic stretching and restoring tests. It can be seen that during the cyclic tests, the mechanical properties of the SPC remain stable, which precisely reflect the characteristics of a superelastic material. Fig. 4b characterizes the nanostructures of the SPC before and after cyclic stretching and restoring tests, from which we can see that the nanostructures of the SPC is basically unchanged. This morphologically reflects the stability of color change performance of the SPC during 2000 cycles of cyclic stretching and restoring tests.

To further characterize the color change performance of the SPC under cyclic stretching, the variation of color range and reflectivity were tested in the cyclic test. Fig. 4c illustrates the reflectance spectra data of the SPC at the strain of 0%, 17%, 30% after 0, 50, 100, 500, 1000 and 2000 times cyclic test, respectively. The spectra were analyzed and the wavelength change Δλ as well as the reflectivity of the band gap were

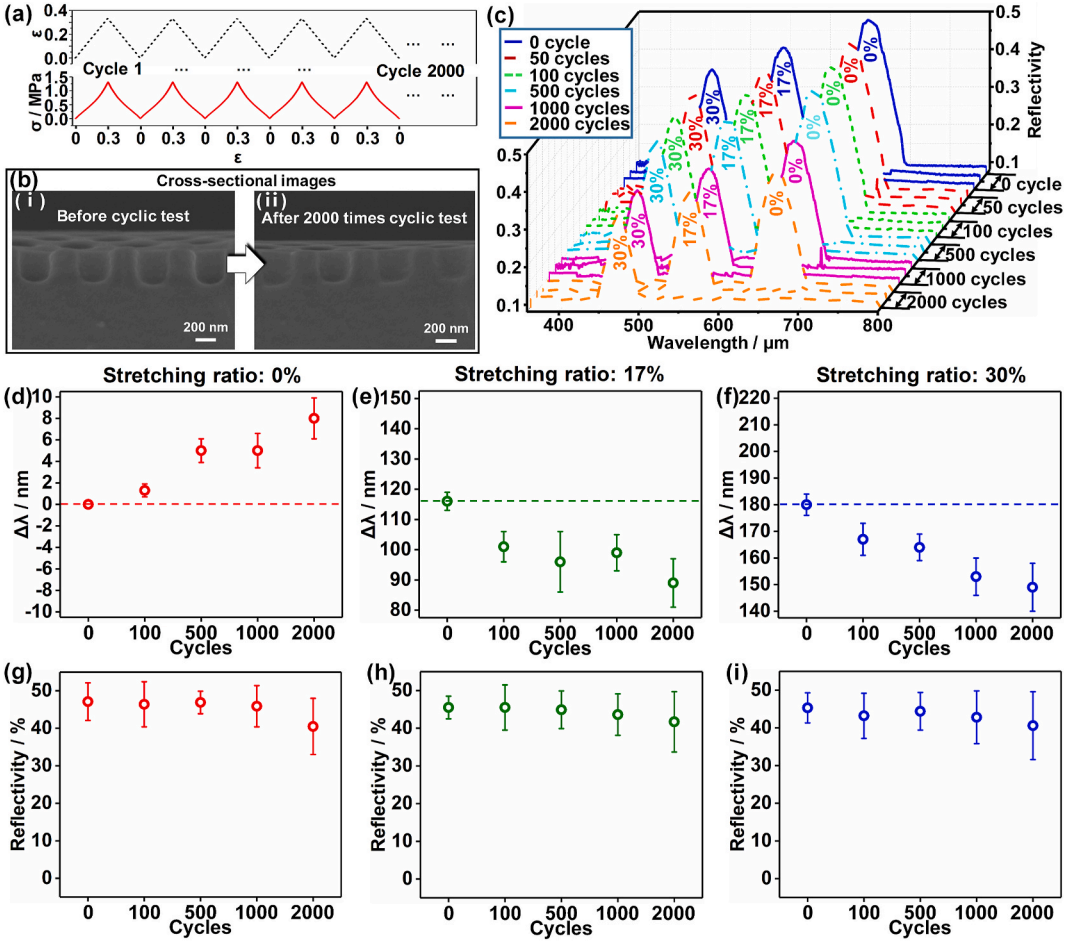

Fig. 4. Color change performance of the SPC under cyclic mechanical stretching. (a) Stress σ, Strain ε of the SPC when cyclic loading and removing the pulling force for 2000 cycles. (b) Nanostructures of the SPC before and after cyclic stretching and restoring tests. (c) Reflectance spectra data of the SPC at the strain of 0%, 17%, 30% after 0, 50, 100, 500, 1000 and 2000 times cyclic test, respectively. (d), (e) and (f) The wavelength change Δλ of the spectral peak at three target strain after cyclic test. The error bars represent the deviations of twelve sets of test data. (g), (h) and (i) The peak value of the reflectance spectra at three target strain after cyclic test. The error bars represent the deviations of twelve sets of test data. (For interpretation of the references to color in this figure legend, the reader is referred to the Web version of this article.)

compared in detail as shown in Fig. 4d ~ i.

Fig. 4d, e and 4f show the variation of central wavelength Δλ of the reflectance spectra at three target strain after cyclic test. The error bars represent the deviations of twelve sets of test data. Despite some changes of wavelength, the variation of central wavelength Δλ of the reflectance spectra remains basically unchanged before and after cyclic test. Fig. 4g, h and 4i shows the peak value of the reflectance spectra at three target strain after cyclic test, respectively. The error bars represent the deviations of twelve sets of test data. It can be seen from the figures that the peak value of reflectivity is relatively stable before and after cyclic test. The series of experimental results reflect that the central wavelength Δλ and the peak value of the reflectance spectra are basically stable within 2000 working cycles, which indicates that the proposed SPC maintain satisfactory color change performance under cyclic mechanical stretching.

3.3. Electrochromic performance of the EDDEA

The sample and structure of EDDEA is shown in Fig. 5a, in which the DEA deform under an applied voltage, causing the strain and color change of the SPC. As shown in Fig. 5a, the color of SPC sample shows red (RGB of central point: 190, 88, 34) before deformation occurring. When a voltage applies on the device, the deformation of actuator will gradually increase and the color of SPC will change accordingly. The yellow color (RGB of central point: 147, 136, 0) of the device corresponds to the strain of 10% in the vertical direction (see Fig. 5b.). The green color (RGB of central point: 73, 142, 0) of the device corresponds to the strain of 17% in the vertical direction (see Fig. 5c.). The blue color (RGB of central point: 10, 143, 190) of the device corresponds to the strain of 30% in the vertical direction (see Fig. 5d.).

Fig. 5e shows the displacement of the free end of EDDEA under applied voltage in the actuating process. The applied voltage increases from 0 V to 6500 V (the increase amplitude for each time ΔU = 500 V). It can be seen that the actuator does not deform below 3500 V. When the applied voltage increases to 3500 V, the significant deformation of DEA occurs. When the applied voltage reaches 6500 V, the deformation of DEA reaches its maximum value (5.9 mm), and then breakdown occurs. The upper left corner of Fig. 5e illustrates the deformation response time of the EDDEA when the applied voltage rises by 500 V instantaneously. It can be seen that when the applied voltage rises instantaneously, the

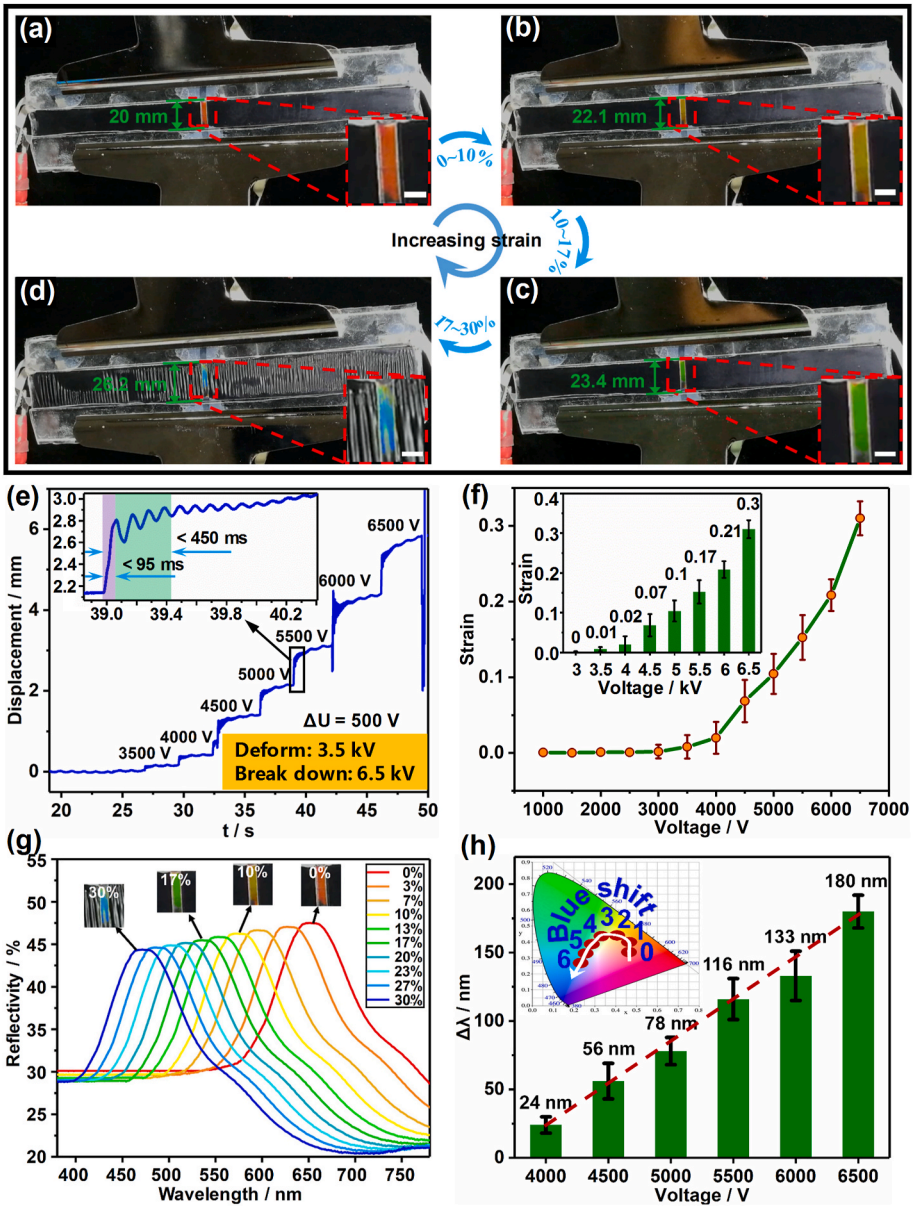

Fig. 5. Electrochromic performance of the EDDEA. (a), (b), (c), and (d) Electrochromic process of the EDDEA under applied voltage. Scale bar is 5 mm. (e) Displacement of the free end of the device under varying voltage from 0 V–6500 V ΔU = 500 V. The upper left corner of the figure illustrates the deformation response time of the EDDEA when the applied voltage rises by 500 V instantaneously. (f) The strain of the EDDEA under the effective voltage range from 3500 V to 6500 V. (g) The variation of the reflectance spectra of the device during electrochromic process. (h) The wavelength change Δλ of the spectral peak of the device under different applied voltage. The error bars represent the deviations of twelve sets of test data. The upper left corner of the figure illustrates the CIE 1931 chromaticity diagram of the color change caused by the electrostrictive deformation. (For interpretation of the references to color in this figure legend, the reader is referred to the Web version of this article.)

EDDEA can complete the main deformation in less than 95 ms, and can enter the next stable state in less than 450 ms. The results show that the prepared EDDEA has a high response speed, which means the response hysteresis of the EDDEA to the applied voltage is very short. Fig. 5f shows the relationship between the strain of EDDEA and the applied voltage. When the applied voltage increases from 0 V to 6500 V, the strain of EDDEA changes from 0% to 30%, among which the effective voltage range for strain generation is 3500 V–6500 V. The error bars represent the deviations of twelve sets of test data. The strains of EDDEA under 5000 V, 5500 V and 6500 V correspond to the situations depicted in Fig. 5b, c and 5d, respectively.

The variation of the reflectance spectra of the EDDEA during electrochromic process is shown in Fig. 5g. The strain of the device gradually changes from 0 to 30% under applied voltage, and the color gradually changes from red to blue accordingly. In addition, the peak value of the reflectance spectra is basically maintained at a stable level during the electrochromic process (see Table S1 in Supporting Information). During the electrochromic process of the EDDEA, the color corresponding to strain of 10% is yellow, the color corresponding to strain of 17% is green, the color corresponding to strain of 30% is blue.

Fig. 5h illustrates the wavelength change $\Delta\lambda$ of the spectral peak of the device under different applied voltage. The error bars are used to represent the deviations of twelve sets of test data. Corresponding to the voltages of 4000, 4500, 5000, 5500, 6000, 6500 V, the wavelength variation $\Delta\lambda$ is 24, 56, 78, 116, 133, 180 nm, among which the largest color change range can cover the whole visible light range. With the increase of the voltage, the strain of the actuator increases gradually, leading to the color change correspondingly. When the strain reaches 10% under the voltage of 5000 V, the color changes from red to yellow. When the strain reaches 17% under the voltage of 5500 V, the color changes from red to green. When the strain reaches 30% under the voltage of 6500 V, the color changes from red to blue. Furthermore, the relationship between applied voltage and color change maintain linear on the whole. The figure in the upper left corner of Fig. 5h shows the variation of CIE 1931 chromaticity of the device in the electrochromic process. It can be seen that the color change caused by the electrostrictive deformation can cover the whole visible light range and there is a quantitative relationship between the applied voltage and the color change range. The experimental results show that the proposed EDDEA has the ability to change color in a wide range with good linearity under applied voltage, and the color change process responds fastly to the variation of voltage.

3.4. Application of the EDDEA in strain sensing

For DEAs, there is a certain relationship between the deformation and the applied voltage, that the deformation increases with the increase of the voltage. However, the traditional DEAs cannot realize the accurate control of deformation under the voltage because of the inconsistencies in the materials and preparation process, which undoubtedly limits its application in the field of flexible manipulator, soft robot, etc. While the design and mechanics of DEAs have improved, they still do not provide quantitative feedback regarding the strain of DEAs. In order to solve this problem, sensors or measuring devices can be added to DEA to get the strain data of the actuator under the applied voltage, and then the data can be compared with the strain limit to guide the actuating process in reverse. Nevertheless, there are some inherent defects of the above scheme in technical implementation. That is, the introducing of sensors, measuring devices, and the software and hardware systems for data processing will increase the complexity of the system as well as the overall weight of the actuator. It can be seen that the proposed EDDEA can judge the strain range according to the colors of the device, and the strain sensing can be realized with a simple structure.

Firstly, we tested and calibrated the strain sensing performance of the SPC. Recently, carbon nanotubes/polydimethylsiloxane (CNTs/PDMS) composites have been widely studied and applied to make soft sensors. Therefore, we choose the CNTs/PDMS composite as a reference to comparatively test and study the strain sensing performance of the SPC in this study. The testing scheme of the comparison of strain sensing capability between the SPC and the CNTs/PDMS composites is shown in Fig. 6a. We prepared a stretchable strain sensor made of CNTs/PDMS composites with CNTs contents of 3 wt% according to reference [75], and attached the prepared SPC to the surface of the sensor to form a double-layer structure (see Fig. 6b.). Then a source meter (Keithley 2450, Cleveland, Ohio, USA) and a tensile testing machine (ZQ-60B) were used to carry out the experiment to comparatively study the strain sensing capability of the two materials. Tensile tests for the prepared double-layer structure were carried out and the relationships between the strain and the resistance of the CNTs/PDMS composite as well as the colors of the SPC during the stretching process are analyzed as shown in Fig. 6c. The upper left corner of the figure defines the sensitivity of the SPC to strain, which is the tangent slope of the curve of relationship between the color and the strain. The sensitivity can be expressed as follows.

$$S_i = \frac{dy}{dx}\Big|_{x=x_i} \tag{1}$$

It can be seen from Fig. 6c that the CNTs/PDMS composites can produce obvious resistance change. However, when the strain is small (<30%, especially < 10%), the sensitivity of the resistance change to the strain is insufficient. Different from the CNTs/PDMS composites, the prepared SPC has good sensitivity under small strain, and can display colors of red, yellow, green and blue successively when the strain changes from 0% to 30%. This sensing performance enables the SPC to provide an effective auxiliary reference for common soft sensors made of CNTs/PDMS composites.

Fig. 6d illustrates the comparison of three indexes of the prepared EDDEA with those of the other existing electrochromic devices actuated by high voltage (>1 kV). The three axes represent the applied voltage, the maximum wavelength change range of the device $\Delta\lambda$ and the maximum output strain of the device. The concrete data of Fig. 6d are listed in Table 1. It can be seen that, compared with other existing electrochromic devices actuated by high voltage, the proposed EDDEA can produce a larger range of color change (up to 180 nm) under the same level of applied voltage, covering the whole visible light range. Furthermore, the EDDEA can output a stretching strain of more than 30% under the applied voltage, which is a unique feature not found in other electrochromic devices. Those properties make it possible for the EDDEA to be used in some special occasions such as the flexible morphing wing that requires strain sensing while providing sufficient actuating deformation.

For comparison to show the strain sensing capability of the device, the EDDEA with SPC and the DEA without SPC were prepared respectively, and the comparison of their strain sensing capability during the actuating process is also shown in Fig. 6. It should be noted that a sheet of soft film with the same material as SPC but no color was fabricated on the DEA without SPC for comparability and the DEA without SPC is controlled through experience. The deviation ranges of the strain of DEA under applied varying voltage of 3500 V, 4000 V, 4500 V, 5000 V, 5500 V, 6000 V and 6500 V were analyzed, the statistical results of 12 groups of test data for strain of DEA are shown in Fig. 6e. Then the data was analyzed and the deviation ranges of strain under each voltage were shown in Fig. 6f. It can be seen that deviation ranges of the strain of DEA under each voltage is about 10% (for specific data see the table in upper left corner of Fig. 6f.). The maximum deviation range is 13.11%, while the minimum deviation range is 5.97%, and the rest deviation range is about 10%. From the above results we can see that the deviation range of strain is relatively large for the traditional DEA which control the strain by controlling the applied voltage according to the experience gained through multiple experiments. In other words, the consistency of strains obtained by the above mentioned method is poor. Therefore, it is

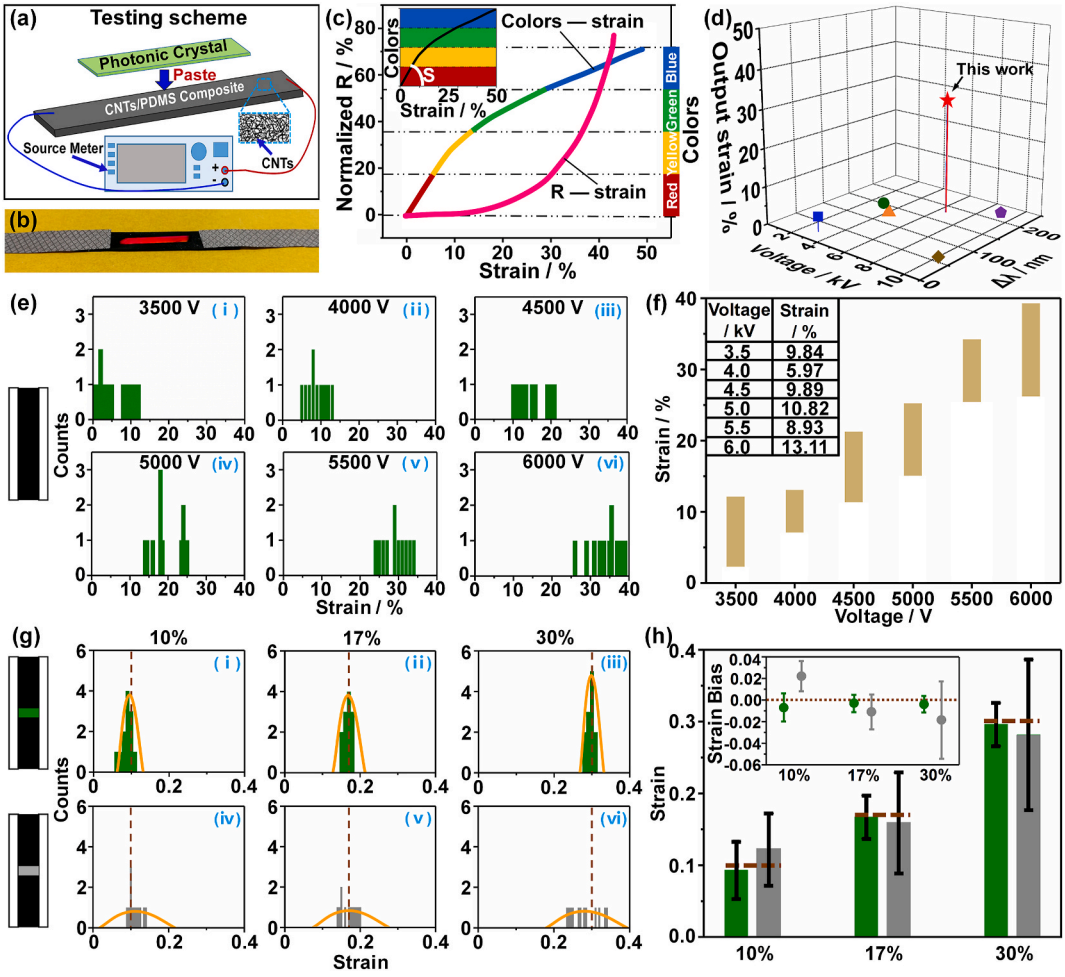

Fig. 6. The strain sensing capability of the proposed EDDEA. (a) The testing scheme of the comparison of strain sensing capability between the SPC and CNTs/PDMS composites. (b) An optical photograph of the sample for the testing scheme in (a). The red and black parts are the SPC as well as the CNTs/PDMS composites, respectively. The silvery part on both sides are the electric conductivity fabrics. (c) The strain sensing capability of the SPC compared with the CNTs/PDMS composites. The upper left corner of the figure defines the sensitivity of the SPC. (d) Comparison of three indexes of the EDDEA with those of the other electrochromic devices actuated by high voltage (>1 kV). (e) Statistical strain data of 12 sets of the DEA under the voltage of 3500 V, 4000 V, 4500 V, 5000 V, 5500 V, 6000 V and 6500 V. (f) The deviation ranges of strain under certain voltages obtained by analyzing the data in (e). (g) Statistical strain data of 12 sets of the EDDEA and the DEA without SPC under the target strain of 10%, 17% and 30%. The green data represents that from EDDEA, and gray data represents that from normal DEA without SPC. The yellow lines represent the normal distribution fit of 12 sets of data under each target strain. The red dotted lines represent the location of each target strain. (h) The deviation ranges of the strain under certain target strain obtained by analyzing the data in (g). The red dotted lines represent the location of each target strain. (For interpretation of the references to color in this figure legend, the reader is referred to the Web version of this article.)

Table 1
Main parameters of the high-voltage (>1 kV) electrochromic devices.

References	Wavelength change range (nm)	Actuating voltage (kV)	Output strain (%)	Symbols
This study	180	6.5	30	★
[24]	150	3	0	●
[42]	130	4	0	▲
[50]	225	9	0	⬟
[76]	60	10	0	◆
[77]	25	3	3.6	■

necessary to improve the strain sensing ability of the actuators.

The strain sensing capability of the EDDEA and DEA without the SPC were compared through twelve sets of experiments, and the data was analyzed as shown in Fig. 6g. In this figure, the green data represents that from EDDEA, and gray data represents that from normal DEA without SPC. The yellow lines represent the normal distribution fit of 12 sets of data under each target strain. The red dotted lines represent the location of each target strain. For the EDDEA, the strain is sensed through the colors of SPC, and then the strain range can be controlled. For the DEA without SPC, the strain is controlled by the applied voltage according to experience. From the statistical data in Fig. 6g, it can be found that the 12 sets of actual strain data of the EDDEA under each target strain has smaller deviations from the target strain than that of the DEA without SPC, and the data consistency is also better.

We further analyzed the above test data, then compared the average values and errors of the test data of the EDDEA with that of DEA under each target strain (see Fig. 6h.). In Fig. 6h, the red dotted lines also represent the location of each target strain, and the color of green and gray represent the EDDEA and the DEA, respectively. This figure reflects that the strain data of EDDEA is more concentrated around each target strain owing to the strain sensing capability. The analysis of strain bias in this figure reveals that the strain data of EDDEA has better consistency, which is also caused by the strain sensing capability. The reason for this phenomenon are analyzed as follows. EDDEAs can control the strain by applied voltage according to the color of SPCs, while DEA can only control the strain by applied voltage according to the experiences. However, for DEAs, the strain of different samples under the same voltage is not exactly the same owing to the instability in materials and

preparation, which leads to the worse performance of DEA in strain control than that of DEASA. In other words, the strain of EDDEA is controlled by applied voltage according to the color of SPCs, which cause the strain data more centralized. While the strain of DEA is controlled by applied voltage according to the experiences, which cause the strain data more discrete.

The experimental results indicates that the EDDEA has good strain sensing capability because it integrated the SPC that can display color changes during deformation. The scheme is a good inspiration for the development of various DEAs with strain sensing capability.

4. Conclusions

In this work, inspired by the skin of chameleons, an electrochromic device enabled via dielectric elastomer actuator (EDDEA) is prepared by integrating the pure shear DEAs with the stretchable photonic crystals (SPCs), which can achieve a wide range of electrochromism under applied voltage. Firstly, a pure shear DEA was prepared and its mechanical properties as well as actuating performance under an electric field are studied. Subsequently, an SPC with hexagonally arranged air columns was prepared, which has the advantages of wide color changing range (180 nm), small Young's Modulus, and good color changing stability (2000 cycles). Based on the properties of the proposed pure shear DEAs and SPCs, the integrated structure of the SPC and DEA was designed and fabricated, obtaining the EDDEA which can produce color change in visible light range from red to blue under an electric field. After that, the electrochromic property of EDDEA was studied and the relationship between applied voltage, strain range, and structural colors was also analyzed. When the voltage ranging from 3.5 kV to 6.5 kV applied to the prepared EDDEA, a strain up to 30% occurred and a wide range of color change came up corresponding to the strain ranges. Finally, the application of the EDDEA was explored in the strain sensing of DEA by a group of comparative experiments, which validates that the strain data of EDDEA is more consistent owing to the strain sensing capability. Our research may not merely produce a new type of electrochromic device, but also provide a new idea for realizing the sensing function of soft actuators.

CRediT authorship contribution statement

Pengfei Zhao: Conceptualization, Data curation. **Yong Cai:** Supervision. **Chen Liu:** Supervision. **Dengteng Ge:** Supervision. **Bo Li:** Supervision. **Hualing Chen:** Supervision.

Declaration of competing interest

The authors declare that they have no known competing financial interests or personal relationships that could have appeared to influence the work reported in this paper.

Acknowledgements

The authors acknowledge the financial support from the National Natural Science Foundation of China (91748124), Scientific and Technological Innovation Programs of Higher Education Institutions in Shanxi (2019L0936) and Basic Scientific Research Project of China in National Defense Bureau. The authors also would like to thank Na Li, Bingshu Zhao and Yueshu Zhao for their kind support of this work and thank Mr. Zijun Ren for SEM images.

Appendix A. Supplementary data

Supplementary data to this article can be found online at https://doi.org/10.1016/j.optmat.2020.110569.

References

[1] E. Acome, S.K. Mithchell, T.G. Morrissey, M.B. Emmett, C. Benjamin, M. King, M. Radakovitz, C. Keplinger, Hydraulically amplified self-healing electrostatic actuators with muscle-like performance, Science 359 (2018) 61–65.
[2] Y.F. Goh, S. Akbari, T. Vo, S.J.A. Koh, Electrically-induced actuation of acrylic-based dielectric elastomers in excess of 500% strain, Soft Robot. 5 (2018) 675–684.
[3] Y. Wang, B.H. Chen, Y.Y. Bai, H. Wang, J.X. Zhou, Actuating dielectric elastomers in pure shear deformation by elastomeric conductors, Appl. Phys. Lett. 104 (2014), 064101.
[4] P. Fan, L.Q. Zhu, H.L. Chen, B. Luo, Energy harvesting from a DE-based soft pendulum, Smart Mater. Struct. 27 (2018) 115023.
[5] P. Fan, H.L. Chen, B. Li, Y.J. Wang, Performance investigation on dissipative dielectric elastomer generators with a triangular energy harvesting scheme, Europhys. Lett. 120 (2017) 47007.
[6] C. Tang, W.T. Ma, B. Li, M.L. Jin, H.L. Chen, Cephalopod-inspired swimming robot using dielectric elastomer synthetic jet actuator, Adv. Eng. Mater. 22 (2019) 1901130.
[7] C. Tang, B. Li, W.J. Sun, Z.Q. Li, H.L. Chen, Identification and characterization of the out-of-plane resonance in a dielectric elastomer to drive an agile robotic cube, J. Appl. Phys. 122 (2017) 165104.
[8] B. Li, H.L. Chen, J. Qiang, S. Hu, Z. Zhu, Y. Wang, Effect of mechanical pre-stretch on the stabilization of dielectric elastomer actuation, J. Phys. Appl. Phys. 44 (2011) 155301.
[9] X. Zhao, W. Hong, Z. Suo, Electromechanical hysteresis and coexistent states in dielectric elastomers, Phys. Rev. B 76 (2007) 134113.
[10] X. Zhao, Z. Suo, Method to analyze electromechanical stability of dielectric elastomers, Appl. Phys. Lett. 91 (2007), 061921.
[11] C. Bolzmacher, J. Biggs, M. Srinivasan, Flexible dielectric elastomer actuators for wearable human-machine interfaces, Smart Structures and Materials 6168 (2006) 616804. Electroactive Polymer Actuators and Devices (EAPAD).
[12] G. Kofod, The static actuation of dielectric elastomer actuators: how does pre-stretch improve actuation, J. Phys. Appl. Phys. 41 (2008) 215405.
[13] J. Huang, T. Lu, J. Zhu, D. Clarke, Z. Suo, Large, uni-directional actuation in dielectric elastomers achieved by fiber stiffening, Appl. Phys. Lett. 100 (2012) 211901.
[14] M. Kollosche, J. Zhu, Z. Suo, G. Kofod, Complex interplay of nonlinear processes in dielectric elastomers, Phys. Rev. 85 (2012), 051801.
[15] P.G. Kang, S.O. Ogunbo, D. Erickson, High resolution reversible color images on photonic crystal substrates, Langmuir 27 (2011) 9676–9680.
[16] T.H. Wu, T.H. Yin, X.C. Hu, G.D. Nian, S.X. Qu, W. Yang, A thermochromic hydrogel for camouflage and soft display, Adv.Opt.Mater. 8 (2020) 2000031.
[17] M.Y. Lin, T.H. Tsai, L.J. Hsiao, W.C. Tu, S.H. Wu, L.A. Wang, S.C. Lee, H.Y. Lin, Design and fabrication of nano-structure for three-dimensional display application, IEEE Photon. Technol. Lett. 28 (2016) 884–886.
[18] K. Hwang, D. Kwak, C. Kang, D. Kim, Y. Ahn, Y. Kang, Electrically tunable hysteretic photonic gels for nonvolatile display pixels, Angew. Chem. Int. Ed. 50 (2011) 6311–6314.
[19] W. Zhang, M. Anaya, G. Lozano, M.E. Calvo, M.B. Johnston, H. Miguez, H.J. Snaith, Highly efficient perovskite solar cells with tunable structural color, Nano Lett. 15 (2015) 1698–1702.
[20] J.J. Walish, Y. Kang, R.A. Mickiewicz, E.L. Thomas, Bioinspired electrochemically tunable block copolymer full color pixels, Adv. Mater. 21 (2009) 3078–3081.
[21] T.S. Shim, S.H. Kim, J.Y. Sim, J.M. Lim, S.M. Yang, Dynamic modulation of photonic bandgaps in crystalline colloidal arrays under electric field, Adv. Mater. 22 (2010) 4494–4498.
[22] I. Lee, D. Kim, J. Kal, H. Baek, D. Kwak, D. Go, E. Kim, C. Kang, J. Chung, Y. Jang, S. Ji, J. Joo, Y. Kang, Quasi-amorphous colloidal structures for electrically tunable full-color photonic pixels with angle-independency, Adv. Mater. 22 (2010) 4973–4977.
[23] T. Heuser, R. Merindol, S. Loescher, A. Klaus, A. Walther, Photonic devices out of equilibrium: transient memory, signal propagation, and sensing, Adv. Mater. 29 (2017) 1606842.
[24] T.H. Yin, T.H. Wu, D.M. Zhong, J.J. Liu, X.J. Liu, Z.L. Han, H.H. Yu, S.X. Qu, Soft display using photonic crystals on dielectric elastomers, ACS Appl. Mater. Interfaces 10 (2018) 24758–24766.
[25] Y. Xie, Y. Meng, W.X. Wang, E. Zhang, J.S. Leng, Q.B. Pei, Bistable and reconfigurable photonic crystals-electroactive shape memory polymer nanocomposite for ink-free rewritable paper, Adv. Funct. Mater. 28 (2018) 1802430.
[26] C. Zhu, W.Y. Xu, L.S. Chen, W.D. Zhang, H. Xu, Z.Z. Gu, Magnetochromatic microcapsule arrays for displays, Adv. Funct. Mater. 21 (2011) 2043–2048.
[27] H. Liu, H. Yang, Y.R. Li, B.X. Song, Y.F. Wang, Z.R. Liu, L. Peng, H. Lim, J. Yoon, W. Wu, Swithable all-dielectric metasurfaces for full-color reflective display, Adv. Opt.Mater. 7 (2019) 1801639.
[28] P.F. Zhao, H.L. Chen, B. Li, H.M. Tian, D.S. Lai, Y. Gao, Stretchable electrochromic devices enabled via shape memory alloy composites (SMAC) for dynamic camouflage, Opt. Mater. 94 (2019) 378–386.
[29] Y.H. Bao, Y. Han, W.L. Song, H.S. Chen, D.N. Fang, Multi-field coupled color-changing devices and structures, Sci. China Technol. Sci. 62 (2019) 1065–1066.
[30] M. Seo, J. Kim, H. Oh, M. Kim, I.U. Baek, K.D. Choi, J.Y. Byun, M. Lee, Printing of highly vivid structural colors on metal substrates with a metal-dielectric double layer, Adv.Opt.Mater. 7 (2019) 1900196.
[31] Y.Q. Xia, B.H. Chen, S. Gao, Y.J. Liu, Z.J. Zeng, M.W. Cao, S.J. Wang, Tough, freestanding, and colorless photonic paper using water as ink, Advanced Materials Interfaces 6 (2019) 1901363.

[32] E. Van Heeswijk, L.T. Yang, N. Grossiord, A.P.H.J. Schenning, Tunable photonic materials via monitoring step-growth polymerization kinetics by structural colors, Adv. Funct. Mater. 30 (2019) 1906833.
[33] Y.X. Dong, A. Bazrafshan, A. Pokutta, F. Sulejmani, W. Sun, J.D. Combs, K. C. Clarke, K. Salaita, Chameleon-inspired strain-accommodating smart skin, ACS Nano 13 (2019) 9918–9926.
[34] J.B. Kim, G.H. Lee, S.H. Kim, Interfacial assembly of amphiphilic tiles for reconfigurable photonic surfaces, ACS Appl. Mater. Interfaces 11 (2019) 45237–45245.
[35] F.F. Liu, S.F. Zhang, X. Jin, W.T. Wang, B.T. Tang, Thermal-responsive photonic crystal with function of color switch based on thermochromic system, ACS Appl. Mater. Interfaces 11 (2019) 39125–39131.
[36] J.J. Yang, W.D. Zhao, Z. Yang, W.L. He, J.X. Wang, T. Ikeda, L. Jiang, Photonic shape memory polymer based on liquid crystalline blue phase films, ACS Appl. Mater. Interfaces 11 (2019) 46124–46131.
[37] X.W. Du, D.S. Hou, X. Li, D.P. Sun, J.F. Lan, J.L. Zhu, W.J. Ye, Symmetric continuously tunable photonic band gaps in blue-phase liquid crystals switched by an alternating current field, ACS Appl. Mater. Interfaces 11 (2019) 22015–22020.
[38] D.T. Ge, X.M. Yang, Z. Chen, L.L. Yang, G.X. Wu, Y. Xia, S. Yang, Colloidal inks from bumpy colloidal nanoparticles for the assembly of ultrasmooth and uniform structural colors, Nanoscale 9 (2017) 17357–17363.
[39] H.N. Kim, D.T. Ge, E. Lee, S. Yang, Multistate and on-demand smart windows, Adv. Mater. 30 (2018) 1803847.
[40] D.T. Ge, E. Lee, L.L. Yang, Y.G. Cho, M. Li, D.S. Gianola, S. Yang, A robust smart window: reversibly switching from high transparency to angle-independent structural color display, Adv. Mater. 27 (2015) 2489–2495.
[41] V. Mohammad, N.K. Andrew, Y.D. Cong, H.Y. Liang, R. Martin, S. Michael, C. Charles, M. Sergei, A.I. Dimitri, V.D. Andrey, S.S. Sergei, Chameleon-like elastomers with molecularly encoded strain-adaptive stiffening and coloration, Science 359 (2018) 1509–1513.
[42] H.K. Chang, J. Park, Flexible all-solid-state electrically tunable photonic crystals, Adv.Opt.Mater. 6 (2018) 1800792.
[43] Y. Tian, J. Zhang, S.S. Liu, S.Y. Yang, S.N. Yin, C.F. Wang, L. Chen, S. Chen, Facile construction of dual bandgap optical encoding matertials with PS@P(HEMA-co-AA)/SiO2-TMPTA colloidal photonic crystals, Opt. Mater. 57 (2016) 107–113.
[44] M.Z. Yang, Y. Liu, X.Y. Jiang, Barcoded point-of-care bioassays, Chem. Soc. Rev. 48 (2019) 850–884.
[45] L.R. Shang, W.X. Zhang, K. Xu, Y.J. Zhao, Bio-inspired interlligent structural color materials, Materials Horizons 6 (2019) 945–958.
[46] C.H. Liu, H.B. Ding, Z.Q. Wu, B.B. Gao, F.F. Fu, L.R. Shang, Z.Z. Gu, Y.J. Zhao, Tunable structural color surfaces with visually self-reporting wettability, Adv. Funct. Mater. 26 (2016) 7937–7942.
[47] T. Lu, W.H. Peng, S.M. Zhu, D. Zhang, Bio-inspired fabrication of stimuli-responsive photonic crystals with hierarchical structures and their applications, Nanotechnology 27 (2016) 122001.
[48] W. Wohlleben, F.W. Bartels, S. Altmann, R.J. Leyrer, Mechano-optical octave-tunable elastic colloidal crystals made from core-shell polymer beads with self-assembly techniques, Langmuir 23 (2007) 2961–2969.
[49] J.D. Sandt, M. Moudio, J.K. Clark, J. Hardin, C. Argenti, M. Carty, J.A. Lewis, M. Kolle, Stretchable optomechanical fiber sensors for pressure determination in compressive medical textiles, Adv.Healthcare.Mater. 7 (2018) 1800293.
[50] D.Y. Kim, S. Choi, H. Cho, J.Y. Sun, Electroactive soft photonic devices for the synesthetic perception of color and sound, Adv. Mater. 31 (2018) 1804080.
[51] H. Lee, J. Kim, H. Kim, J. Kim, S. Kwon, Colour-barcoded magnetic microparticles for multiplexed bioassays, Nat. Mater. 9 (2010) 745–749.
[52] Y.P. Wang, W.B. Niu, S.F. Zhang, B.Z. Ju, Solvent responsive single-material inverse opal polymer actuator with structural color switching, J. Mater. Sci. 55 (2020) 817–827.
[53] J.Y. Chen, L.R. Xu, M.J. Yang, X.C. Chen, X.D. Chen, W. Hong, Highly stretchable photonic crystal hydrogels for a sensitive mechanochromic sensor and direct ink writing, Chem. Mater. 31 (2019) 8918–8926.
[54] M. Qin, M. Sun, R.B. Bai, Y.Q. Mao, X.S. Qian, D. Sikka, Y. Zhao, H.J. Qi, Z.G. Suo, X.M. He, Bioinspired hydrogel interferometer for adaptive coloration and chemical sensing, Adv. Mater. 30 (2018) 1800468.
[55] W. Peng, H. Wu, Flexible and stretchable photonic sensors based on modulation of light transmission, Adv.Opt.Mater. 7 (2019) 1900329.
[56] P.F. Zhao, B. Xu, Y.K. Zhang, B. Li, H.L. Chen, Study on the twisted and coiled polymer actuator with strain self-sensing ability, ACS Appl. Mater. Interfaces 12 (2020) 15716–15725.
[57] R. Hong, Y.Q. Shi, X.Q. Wang, L. Peng, X.J. Wu, H.Y. Cheng, S. Chen, Highly sensitive mechanochromic photonic gel towards fast-responsive fingerprinting, RSC Adv. 7 (2017) 33258–33262.
[58] A. Belmonte, Y.Y. Ussembayev, T. Bus, I. Nys, K. Neyts, A.P.H.J. Schenning, Dual light and temperature responsive micrometer-sized structural color actuators, Small 16 (2019) 1905219.
[59] Y. Jin, Y.L. Lin, A. Kiani, I.D. Joshipura, M.Q. Ge, M.D. Dickey, Materials tactile logic via innervated soft thermochromic elastomers, Nat. Commun. 10 (2019) 4187.
[60] Q.L. Zhao, Y.L. Wang, H.Q. Cui, X.M. Du, Bio-inspired sensing and actuating materials, J. Mater. Chem. C 7 (2019) 6493–6511.
[61] K. Nickmans, D.A.C. Van der Heijden, A.P.H.J. Schenning, Photonic shape memory chiral nematic polymer coatings with changing surface topography and color, Adv. Opt.Mater. 7 (2019) 1900592.
[62] P. Snapp, P. Kang, J. Leem, S. Nam, Colloidal photonic crystal strain sensor integrated with deformable graphene phototransducer, Adv. Funct. Mater. 29 (2019) 1902216.
[63] Y.J. Quan, M.S. Kim, Y. Kim, S.H. Ahn, Colour-tunable 50% strain sensor using surface-nanopatterning of soft materials via nanoimprinting with focused ion beam milling process, CIRP Ann. - Manuf. Technol. 68 (2019) 595–598.
[64] P.F. Zhao, B. Li, Z.H. Tang, Y. Gao, H.M. Tian, H.L. Chen, Stretchable photonic crystals with inverse cylinder periodic nanostructures for improving mechanochromic performance, Smart Mater. Struct. 28 (2019), 075037.
[65] S.C. Niu, B. Li, Z.Z. Mu, M. Yang, J.Q. Zhang, Z.W. Han, L.Q. Ren, Excellent structure-based multifunction of morpho butterfly wings: a review, JBE 12 (2015) 170–189.
[66] F.F. Fu, L.R. Shang, Z.Y. Chen, Y.R. Yu, Y.J. Zhao, Bioinspired living structural color hydrogels, Science Robotics 3 (2018) eaar8580.
[67] J. Teyssier, S.V. Saenko, D. Van der marel, M.C. Milinkovitch, Photonic crystals cause active colour change in chameleons, Nat. Commun. 6 (2015) 6368.
[68] Z.Y. Chen, F.F. Fu, Y.R. Yu, H. Wang, Y.X. Shang, Y.J. Zhao, Cardiomyocytes-actuated morpho butterfly wings, Adv. Mater. 31 (2019) 1805431.
[69] M. Yao, J.J. Qiu, S.L. Wu, B.Z. Ju, S.F. Zhang, B.T. Tang, Biomimetic structural color films with a bilayer inverse heterostructure for anticounterfeiting applications, ACS Appl. Mater. Interfaces 10 (2018) 38459–38465.
[70] V. Sharma, M. Crne, J.O. Park, M. Srinivasarao, Structural origin of circularly polarized iridescence in jeweled beetles, Science 325 (2009) 449–451.
[71] V. Saranathan, C.O. Osuji, S.G.J. Mochrie, H. Noh, S. Narayanan, A. Sandy, E. R. Dufresne, R.O. Prum, Structure, function, and self-assembly of single network gyroid (I4(1)32) photonic crystals in butterfly wing scales, Proc. Natl. Acad. Sci. U. S.A. 107 (2010) 11676–11681.
[72] V. Piccolo, A. Chiappini, C. Armellini, M. Barozzi, A. Lukowiak, P.J.A. Sazio, A. Vaccari, M. Ferrari, D. Zonta, 2D optical gratings based on hexagonal voids on transparent elastomeric substrate, Micromachines 9 (2018) 345.
[73] V. Piccolo, A. Chiappini, C. Armellini, M. Mazzola, A. Lukowiak, A. Seddon, M. Ferrari, D. Zonta, Quasi-hemispherical voids micropatterned PDMS as strain sensor, Opt. Mater. 86 (2018) 408–413.
[74] B. Li, P.F. Zhao, W.T. Ma, Y. Sun, H.L. Chen, G.M. Chen, Mechanochromics of stretchable nano metasurfaces: non-close-packed hexagonal lattices and tunable structural coloration, APEX 13 (2020), 015008.
[75] Z.H. Tang, S.H. Jia, F. Wang, C.S. Bian, Y.Y. Chen, Y.L. Wang, B. Li, Highly stretchable core-sheath fibers via wet-spinning for wearable strain sensors, ACS Appl. Mater. Interfaces 10 (2018) 6624–6635.
[76] Q.B. Zhao, A. Haines, D. Snoswell, C. Keplinger, R. Kaltseis, S. Bauer, I. Graz, R. Denk, P. Spahn, G. Hellmann, J.J. Baumberg, Electric-field-tuned color in photonic crystal elastomers, Appl. Phys. Lett. 100 (2012) 101902.
[77] J.Q. Xia, Y.R. Ying, S.H. Foulger, Electric-field-induced rejection wavelength tuning of photonic bandgap composites, Adv. Mater. 17 (2005) 2463–2467.